MSI Journal of AI and Technology

Volume: 2, Issue: 4 (Oct-Dec 2026)
Published by *MSI Publishers*
ISSN 3107-6181 (Online)

Received: 19-10-2026
Accepted: 10-11-2026
Published: 18-11-2026

Modelling and Simulation of Fouling in a Shell-and-Tube Heat Exchanger for Performance Improvement: An ANSYS-Based Case Study

Authors Details

Francis Chimobi Akpa[1*]
Department of Mechanical Engineering, Faculty of Engineering, University of Port Harcourt, Port Harcourt, Rivers State, Nigeria.

Prof. C. V. Ossia[2]
Department of Mechanical Engineering, Faculty of Engineering, University of Port Harcourt, Port Harcourt, Rivers State, Nigeria.

Corresponding Author: *Francis Chimobi Akpa*

ABSTRACT: Fouling on heat transfer surfaces lowers the thermal efficiency of shell-andtube heat exchangers, increases energy consumption and causes unplanned shutdowns in oil and gas processing. This study modelled and simulated fouling in a horizontal BEMtype shell-and-tube exchanger (TEMA standard, 64 stainless-steel tubes) that cools a hydrocarbon stream with water at an oil and gas facility in Bonny Island, Nigeria. The exchanger was modelled and its steady-state operation simulated in ANSYS 14.0 using the facility's design and operating data. Fouling behaviour was assessed over twelve simulated monthly cases, with fouling resistance (R_f) calculated from the clean and fouled overall heat transfer coefficients. In the first month, fouling reduced heat duty by 36.25% relative to the clean exchanger and the overall heat transfer coefficient (U) fell from 26.26–27.02 to 16.15 W/m²·°C. Over the twelve cases, R_f rose from 0.0238 to 0.0264 m²·°C/W while U fell to 15.24 W/m²·°C. Regression showed that R_f was strongly related to U (power law, $R^2 = 0.986$), time (power law, $R^2 = 0.951$) and mass flow rate (logarithmic, $R^2 = 0.902$), and more weakly

DOI: 10.5281/zenodo.24330546

to log mean temperature difference (linear, R^2 = 0.777). Because mass flow rate and time were varied together, their effects could not be separated. The relationships offer a simple basis for forecasting fouling growth and planning cleaning, but they are model-based and require validation against measured plant data.

Keywords: *Fouling; Shell-and-tube heat exchanger; ANSYS; Heat Transfer Performance; Fouling Resistance; Regression Modelling*

1. Introduction

Heat exchangers transfer thermal energy from a hot fluid to a cold fluid across a separating surface and are integral to oil and gas processing, power generation, chemical production and many other industries (Anand, 2023; Wu et al., 2019; Yang et al., 2020). Of the available types, the shell-and-tube design is the most common in oil and gas processing, because it tolerates high pressures and temperatures and is mechanically robust (Fernandes & Krishanmurthy, 2022; Paul, 2019). It consists of a bundle of tubes enclosed in a cylindrical shell, together with channel heads, tube sheets, baffles, tie rods and spacers. One fluid flows through the tubes while the other flows across them in the shell (Paul, 2019).

The performance of a shell-and-tube exchanger is progressively degraded by fouling, the unwanted accumulation of deposits on heat transfer surfaces (Ogbonnaya & Ajayi, 2017; Sharma & Macchietto, 2021). Deposits form through sedimentation, crystallisation, chemical reaction, biological growth, corrosion or combinations of these mechanisms (Jradi et al., 2022b). Because fouling layers conduct heat poorly, they add thermal resistance, lower the overall heat transfer coefficient, narrow the flow passage, increase pressure drop and pumping power, and, in severe cases, force unplanned shutdowns for cleaning (Kazi, 2020; Tutpol et al., 2023). Fouling costs are substantial: total foulingrelated costs in major industries have been estimated at more than US$4.4 billion annually, and heat exchangers and boilers account for roughly 15% of process-plant maintenance expenditure, much of it attributable to fouling (Ben-Mansour et al., 2023).

Because fouling deposits are time dependent and their thickness and thermal conductivity are rarely known, design and operating practice normally represents them through a fouling resistance (or fouling factor), R_f, which is added to the heat transfer calculation (Jradi et al., 2022b; Müller-Steinhagen, 2011). Fouling models, whether mechanistic, semiempirical or

data driven, estimate R_f at different operating conditions and support cleaning schedules (Loyola, 2019; Rehman et al., 2023; Sundar et al., 2020). Numerical simulation complements them by allowing the effect of operating parameters on exchanger performance to be examined without interrupting plant operation.

1.1 Problem Statement and Research Gap

Fouling in shell-and-tube exchangers is a chronic and largely unresolved operational problem in oil and gas facilities. Cleaning and repair costs, lost throughput and additional energy consumption can be substantial, and unplanned shutdowns are among the largest monetary losses for process operators (Ogbonnaya & Ajayi, 2017). A large body of work has modelled fouling in plate, finned-tube, double-pipe and laboratory-scale exchangers, or has applied statistical and machine-learning methods to monitoring data (Jradi et al., 2022a; Nadra et al., 2020; Ogbonnaya et al., 2020; Sundar et al., 2020; Zahid et al., 2016). Model-based monitoring of in-service shell-and-tube exchangers using plant temperature and pressure-drop data has also been developed (Diaz-Bejarano et al., 2020). However, relatively little attention has been paid to combining a three-dimensional thermal-flow simulation of an in-service shell-and-tube exchanger with simple regression relationships that relate fouling resistance to measurable operating parameters, in a form that operators can use to forecast fouling and plan maintenance.

1.2 Aim and Objectives

The aim of this study was to model and simulate fouling in a shell-and-tube heat exchanger in operation, for performance improvement. The specific objectives were to:

(i) model the design parameters of the exchanger

(ii) simulate its operation using the plant operating parameters

(iii)assess its fouling behaviour at different operating parameters

(iv) develop relationships that describe and predict fouling resistance.

1.3 Significance

The study provided engineers and plant operators with a documented simulation workflow and simple fouling-growth relationships for a typical hydrocarbon cooler. Such relationships

can support the planning of cleaning interventions, longer failure-free operation, higher availability, lower maintenance cost and longer equipment life, and they provide a reference for further research on fouling in shell-and-tube exchangers.

2. Literature Review

2.1 Fouling Mechanisms and Types

Fouling is commonly classified by its dominant mechanism into particulate fouling, chemical-reaction fouling, biological fouling (biofouling), corrosion fouling, crystallisation (scaling) fouling and mixed fouling (Jradi et al., 2022b). Particulate fouling results from the settling of suspended solids such as clay, oxides and carbon residues. Chemicalreaction fouling arises when reactions in the process stream, such as polymerisation, cracking or asphaltene precipitation, form deposits, and it is particularly relevant to hydrocarbon streams. Biofouling is the colonisation of surfaces by micro- and macroorganisms, mainly in aqueous systems. Corrosion fouling occurs when the surface itself reacts with the fluid, and crystallisation fouling is the precipitation of dissolved salts, typically from supersaturated solutions at heated surfaces. In practice, several mechanisms usually act together, with one dominating (Jradi et al., 2022b).

Fouling is a net process in which deposition and removal occur simultaneously. Deposition involves induction (initiation), transport of foulants to the wall (by diffusion, thermophoresis, gravitational settling, inertial impaction or turbulent transport) and attachment, whereas removal occurs through shear, turbulent bursts, re-dissolution and erosion; deposit ageing then alters deposit strength (Jradi et al., 2022b). The net deposition rate, and hence the rate of increase in fouling resistance, is the difference between the deposition and removal rates (Kern & Seaton, 1959).

2.2 Factors Influencing Fouling

The principal influences on fouling are operating parameters, exchanger design and fluid properties (Jradi et al., 2022b). Among operating parameters, fluid velocity and surface and bulk temperatures are most important. Higher velocity raises wall shear stress and generally enhances removal, lowering fouling rate, although in diffusion-controlled processes it can raise deposition. Surface temperature can increase, reduce or leave unchanged the fouling rate depending on the mechanism; for inverse-solubility salts and chemical-reaction fouling,

higher wall temperature increases fouling. Design parameters include surface material, roughness, exchanger type and geometry. Roughness reduces induction time and promotes nucleation and attachment. Fluid properties, including impurities, dissolved species and water quality, can trigger or accelerate deposition (Jradi et al., 2022b).

2.3 Fouling Models and Related Studies

Fouling models range from asymptotic and threshold models to mechanistic, probabilistic and data-driven approaches. In the asymptotic model of Kern and Seaton (1959), R_f approaches a limiting value as deposition and removal balance, and this approach and the TEMA fouling resistances have formed the basis of most fouling models and exchanger designs (Müller-Steinhagen, 2011). Threshold models relate the fouling rate to Reynolds number and wall temperature (Ishiyama et al., 2020). Time-dependent forms have been expressed as linear, logarithmic, exponential or power-law functions of time (Pullela et al., 2020). More recently, neural-network and deep-learning approaches have predicted fouling resistance from routine process measurements with high accuracy (Jradi et al., 2022a; Nadra et al., 2020; Sundar et al., 2020). Table 1 summarises representative studies and indicates where the present work fits.

Table 1 *Representative Studies on Fouling Modelling and Prediction*

Study	Exchanger / approach	Main finding
Zahid et al. (2016)	Laboratory concentric-tube exchanger with a saline system; dynamic model based on Kern–Seaton	Predicted outlet temperatures with average discrepancies of 1.6 °C (cold) and 0.4 °C (hot stream)
Lebele-Alawa & Innocent (2020)	Three exchangers in a polyethylene plant; plant monitoring data	Overall heat transfer coefficient up to 51.6% (cooler) and 80.7% (condenser) below design values
Ogbonnaya et al. (2020)	Plate-and-frame crude-oil cooler; three years of plant data	Fouling resistance rose with time and efficiency fell; lower hot-stream approach temperature gave higher fouling
Pullela et al. (2020)	Analytical study of tube fouling in parallel and counter-flow exchangers	Logarithmic, exponential and power-law time variation of fouling factor; critical maintenance period estimated

Sundar et al. (2020)	Deep-learning prediction for a cross-flow waste-heat exchanger	Mean absolute errors below 10^{-4} K/W and R^2 above 99% for fouling resistance
Diaz-Bejarano et al. (2020)	Dynamic thermo-hydraulic models applied to plant data from heat exchangers	Practical tool for monitoring exchanger performance and early fouling diagnosis
Jradi et al. (2022a)	Artificial neural network for tube-side fouling resistance in a shell-and-tube exchanger	Predicted tube-side fouling resistance from operating data
Swanand & Ashish (2021)	CFD (ANSYS CFX) of baffle cut and spacing in a shell-andtube exchanger	Shell-side heat transfer coefficient increased 13.1–23.1% with more baffles, at the cost of higher pressure drop
Present study	ANSYS simulation of an inservice BEM shell-and-tube exchanger; regression of R_f	Fouling resistance related to U, time, mass flow rate and LMTD

Note. Compiled from the cited studies.

Two gaps emerge. First, most studies address plate, double-pipe, finned-tube or laboratoryscale systems, or rely on monitoring data alone; reviews also note that few results are based on in-situ measurements of real service performance (Ogbonnaya & Ajayi, 2017). Second, few studies couple a three-dimensional thermal-flow simulation of an in-service shell-and-tube exchanger with simple, transparent regression relationships for fouling resistance. The present study addresses this combination.

3. Materials and Methods

3.1 Case Exchanger and Data

The case study was a horizontal BEM-type shell-and-tube heat exchanger (TEMA standard) in continuous service at an oil and gas processing facility in Bonny Island, Rivers State, Nigeria. Its purpose is to cool a stabilised hydrocarbon stream, using water as coolant, to a temperature low enough to limit flashing of light ends in storage tanks and to protect the tank's internal coating. The hydrocarbon flows through the tubes and the cooling water through the shell. Design specifications and design process parameters were obtained from the facility and are given in Tables 2 and 3.

Table 2 *Design Specification of the Shell-and-Tube Heat Exchanger*

Specification	Value	Specification (continued)
Type / standard	BEM, horizontal / TEMA	Tube outside diameter: 19.05 mm
Material	Stainless steel 304	Tube wall thickness: 0.5 mm
Safety factor	2	Number of tubes: 64
Yield strength	205 MPa	Tube length: 2 m
Allowable stress	102 MPa	Baffle type / cut: segmental / 25%
Shell diameter	273.1 mm	Number of baffles: 4
Shell thickness	3.4 mm	Number of tie rods / diameter: 4 / 9.5 mm
Tube-sheet diameter / thickness	266.3 mm / 19.1 mm	

Note. Source: facility design data.

Table 3 *Design Process Parameters*

Parameter	Value
Hydrocarbon mass flow rate (tube side)	248.36 kg/s
Cooling-water mass flow rate (shell side)	127.96 kg/s
Hydrocarbon inlet / outlet temperature	81.1 °C / 48.9 °C
Water inlet / outlet temperature	22.2 °C / 33.3 °C
Hydrocarbon velocity	0.615 m/s
Water velocity	0.325 m/s

Note. Source: facility design data.

3.2 Thermal Analysis

Thermal performance was analysed with the log mean temperature difference (LMTD) method, which is appropriate when inlet temperatures and flow rates are specified. At steady state, the heat released by the hot stream equals that gained by the cold stream, and the duty is related to the exchanger geometry through the overall heat transfer coefficient:

$$Q = U\,A\,\Delta T_{\mathrm{LM}} \tag{1}$$

$$\Delta T_{\mathrm{LM}} = (\Delta T_1 - \Delta T_2) / \ln(\Delta T_1 / \Delta T_2) \tag{2}$$

$$Q = \dot{m}_{\mathrm{c}}\, c_{\mathrm{p,c}}\, (T_{\mathrm{c,out}} - T_{\mathrm{c,in}}) = \dot{m}_{\mathrm{h}}\, c_{\mathrm{p,h}}\, (T_{\mathrm{h,in}} - T_{\mathrm{h,out}}) \tag{3}$$

where Q is heat duty (W), U is the overall heat transfer coefficient (W/m²·°C), A is heat transfer area (m²), $\Delta T_1 = T_{h,in} - T_{c,out}$ and $\Delta T_2 = T_{h,out} - T_{c,in}$ for counter-flow, $\dot{m}$ is mass flow rate (kg/s) and c_p is specific heat (J/kg·°C); subscripts h and c denote the hot and cold streams.

3.3 Fouling Resistance and Heat Transfer Efficiency

Fouling adds a thermal resistance in series with the clean-surface resistances. The clean overall coefficient, referenced to the outside tube area, is

$$U_{cl} = [\ (1/h_i)(D_o/D_i) + 1/h_o + R_w\ ]^{-1} \tag{4}$$

where h_i and h_o are the inside and outside film coefficients, D_o and D_i are the outside and inside tube diameters and R_w is the tube-wall resistance. The service (fouled) coefficient follows from the duty and LMTD:

$$U_s = Q / (A\ \Delta T_{LM}) \tag{5}$$

The fouling resistance is the additional resistance of the fouled exchanger relative to the clean one (Zahid et al., 2016):

$$R_f = 1/U_s - 1/U_{cl} \tag{6}$$

Heat transfer efficiency may be defined as the ratio of service to clean coefficients, $\eta = U_s/U_{cl}$. Because this ratio can mask early fouling, R_f was monitored directly. In the asymptotic Kern–Seaton model, fouling resistance grows towards a limiting value R_f^* as

$$R_f(t) = R_f^*\ [\ 1 - \exp(-t/t_c)\ ] \tag{7}$$

where t is time and t_c is a time constant (Kern & Seaton, 1959; Zahid et al., 2016). The following assumptions were made: no condensation, no leakage, no heat loss to the surroundings and constant tube diameter.

3.4 Geometry, Meshing and Numerical Simulation

The exchanger was modelled in ANSYS 14.0 (Lee, 2017) from the specification in Table 2. The work comprised three stages: construction of the geometry (shell, tubes, baffles, tie rods, tube sheets and nozzles), discretisation of the fluid and solid domains into an unstructured mesh, and steady-state thermal-flow simulation. The mesh was generated as a compromise

between solution time and mesh quality. The simulation applied the flow rates, inlet temperatures, velocities and pressures of Table 3 at the corresponding inlets and outlets, and returned the temperature, pressure and velocity fields, the tube-side outlet temperature and the heat duty. LMTD, U and R_f were then computed from Eqs. 1–6.

3.5 Simulation of Fouling Over Time and Regression Analysis

Fouling behaviour was simulated as twelve successive monthly cases. Starting from the design cooling-water mass flow rate of 127.96 kg/s, the mass flow rate was increased by 10 kg/s in each successive case, and the corresponding hydrocarbon velocity, tube-side outlet temperature, heat duty, LMTD, U and R_f were obtained. The cases therefore represent a simulated progression of operation, not measured plant history.

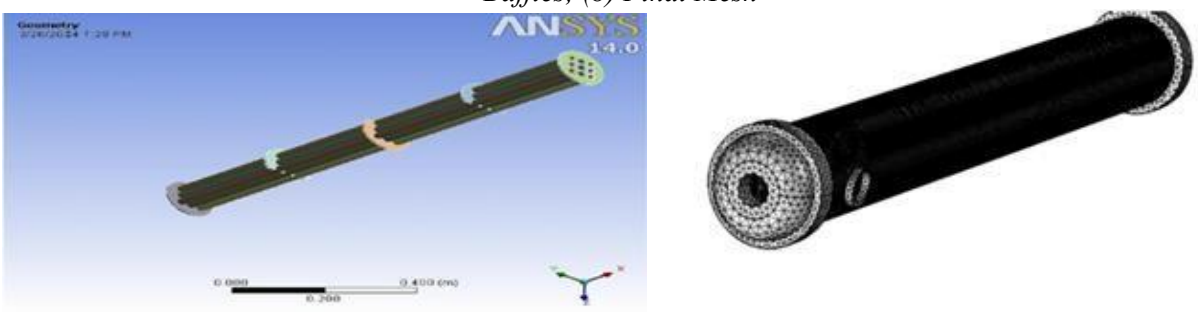
Relationships between R_f and each of U, LMTD, mass flow rate and time were examined by single-variable regression. Linear ($y = b_0 + b_1x$), power ($y = ax^{<i>b</i>}$) and logarithmic ($y = a \ln x + b$) forms were fitted by ordinary least squares (power models after log transformation of both variables) and judged by the coefficient of determination (R^2), the significance of the slope and its 95% confidence interval. The Pearson correlation coefficient (r) was also computed.

4. Results and Discussion

4.1 Exchanger Model and Simulated Fields

Figure 1 shows the assembled exchanger geometry, with the shell, tube bundle and four segmental baffles, and the final computational mesh. Figures 2 and 3 show the simulated temperature and static pressure distributions on a longitudinal section.

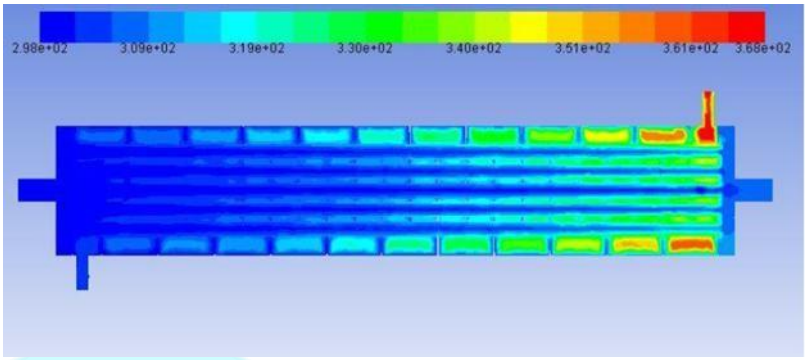
Figure 1 *ANSYS Model of the Shell-and-Tube Heat Exchanger: (a) Assembled Tube Bundle and Baffles; (b) Final Mesh*



Note. Screenshots from ANSYS 14.0.

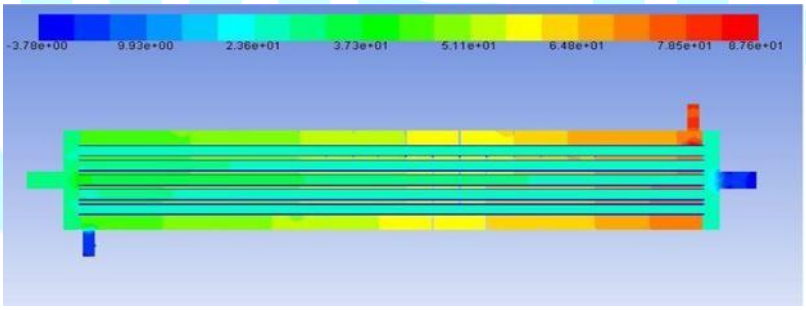
The temperature field (Figure 2) is non-uniform along the exchanger length, with the highest temperatures near the hot-fluid inlet end and lower temperatures towards the opposite end, reflecting progressive heat transfer to the cooling water. The pressure field (Figure 3) shows the highest static pressure near the inlet end, decreasing along the exchanger in the flow direction, as expected from frictional and baffle losses.

Figure 2 *Simulated Temperature Distribution on a Longitudinal Section*



Note. Temperature in K (colour bar).

Figure 3 *Simulated Static Pressure Distribution on a Longitudinal Section*



Note. Pressure values as reported by the solver output (colour bar).

4.2 Fouling Behaviour at Different Operating Parameters

Table 4 gives the simulated fouling behaviour for the twelve monthly cases. Over this period, R_f increased from 0.0238 m²·°C/W in month 1 to 0.0264 m²·°C/W in month 12, an increase of about 11%. Over the same period, the overall heat transfer coefficient decreased from 16.15 to 15.24 W/m²·°C, the tube-side (hydrocarbon) outlet temperature rose from 74.2 °C to 78.9 °C, the simulated heat duty fell from 0.255 to 0.2447 kW, and the hydrocarbon velocity fell slightly from 0.615 to 0.593 m/s, consistent with a progressively narrowed flow passage.

Table 4 *Simulated Fouling Behaviour of the Shell-and-Tube Heat Exchanger over Twelve Monthly Cases*

Month	$\dot{m}$ (kg/s)	v (m/s)	Q (kW)	$T_{h,out}$ (°C)	LMTD (°C)	U (W/m²·°C)	R_f (m²·°C/W)
1	127.96	0.615	0.255	74.20	55.40	16.15	0.023832
2	137.96	0.613	0.254	74.16	55.40	16.09	0.023978
3	147.96	0.611	0.253	78.00	56.35	15.75	0.025192
4	157.96	0.609	0.252	78.10	56.35	15.69	0.025342
5	167.96	0.607	0.251	78.20	56.35	15.63	0.025493
6	177.96	0.605	0.2504	78.30	56.35	15.59	0.025544
7	187.96	0.603	0.249	78.40	56.35	15.50	0.025801
8	197.96	0.601	0.248	78.50	56.35	15.44	0.025957
9	207.96	0.599	0.2473	78.60	56.35	15.40	0.026036
10	217.96	0.597	0.246	78.70	56.35	15.32	0.026274
11	227.96	0.595	0.245	78.80	56.35	15.26	0.026435
12	237.96	0.593	0.2447	78.90	56.35	15.24	0.026409

Note. $\dot{m}$ = cooling-water mass flow rate; v = hydrocarbon velocity; Q = simulated heat duty; $T_{h,out}$ = hydrocarbon (tube-side) outlet temperature; LMTD = log mean temperature difference; $R_f = 1/U_s - 1/U_{cl}$. Values are those of the simulated model.

Comparison with the clean exchanger

Table 5 compares the clean and fouled exchanger in the first monthly case. The fouled exchanger delivered a heat duty of 0.255 kW against 0.400 kW for the clean exchanger (a 36.25% reduction) and cooled the hydrocarbon only to 74.2 °C instead of 70.5 °C, so its hydrocarbon temperature drop was about 35% smaller. The overall heat transfer coefficient fell from 26.26–27.02 W/m²·°C in the clean condition to 16.15 W/m²·°C, a reduction of roughly 38% relative to the lower clean value. This is the expected thermal signature of fouling: an added resistance layer lowers U, reduces duty and raises the outlet temperature of the hot stream, so that either more cooling duty or more heat transfer area would be needed to achieve the same cooling.

Table 5 *Clean and Fouled Exchanger in the First Monthly Case*

Quantity	Clean	Fouled (month 1)
Heat duty, Q (kW)	0.400	0.255
Hydrocarbon outlet temperature (°C)	70.5	74.2
Overall heat transfer coefficient, U (W/m²·°C)	26.26–27.02	16.15
Fouling resistance, R_f (m²·°C/W)	0 (by definition)	0.0238

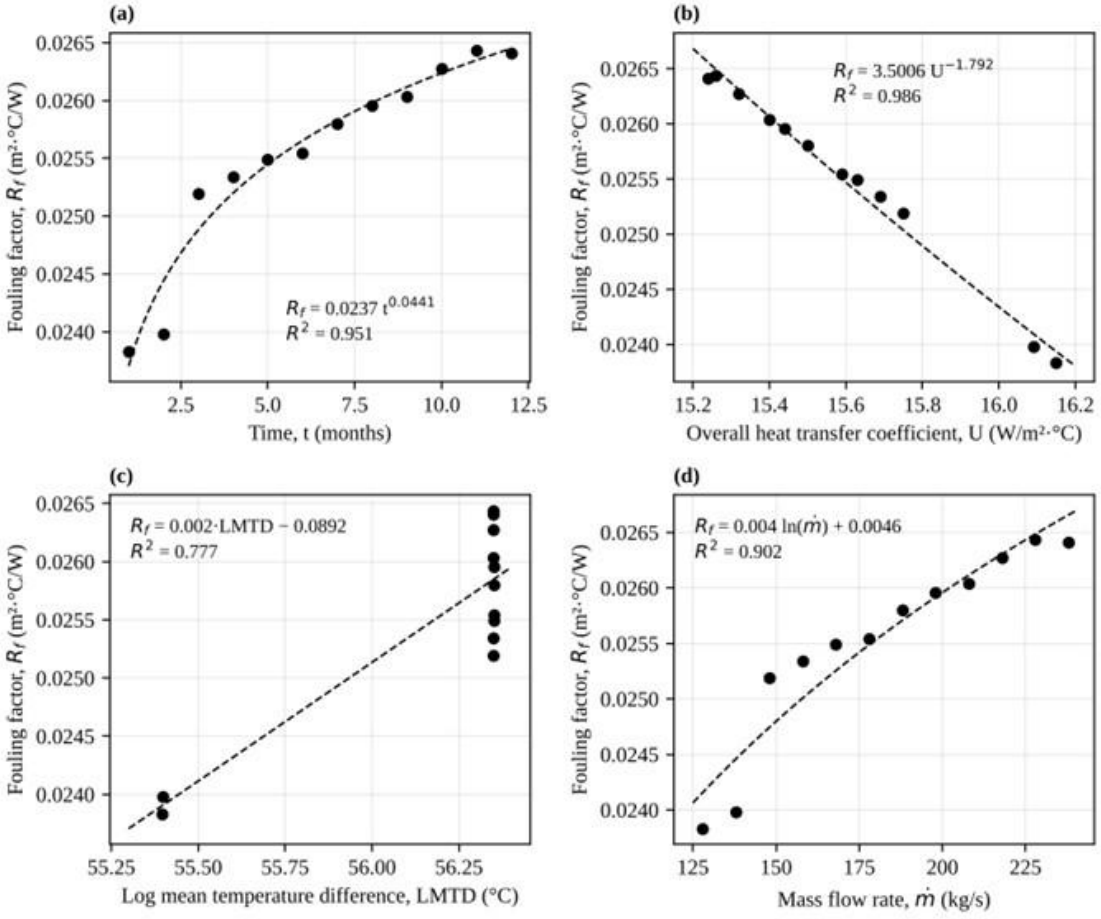
Note. Simulated values. The reduction in heat duty is 36.25%.

LMTD was slightly higher in the fouled than in the clean condition. This follows from the smaller heat transfer and higher hydrocarbon outlet temperature of the fouled exchanger; it is not an indication of better performance, because a higher LMTD accompanying a lower duty indicates a lower effectiveness.

Regression relationships

Figure 4 and Table 6 present the regression relationships. Fouling resistance was most strongly related to the overall heat transfer coefficient, as expected from Eq. 6: a powerlaw relationship, $R_f = 3.5006U^{-1.792}$, explained 98.6% of the variance ($R^2 = 0.986$; Pearson r between R_f and $U = -0.996$). Fouling resistance increased with time following a power law, $R_f = 0.0237t^{0.0441}$ ($R^2 = 0.951$), a decelerating growth pattern that is qualitatively consistent with the asymptotic behaviour represented by the Kern–Seaton model (Eq. 7) and with the power-law time dependence discussed by Pullela et al. (2020).

Figure 4 *Relationships Between Fouling Resistance and (a) Time, (b) Overall Heat Transfer Coefficient, (c) Log Mean Temperature Difference and (d) Mass Flow Rate*



Note. Points are simulated values from Table 4; dashed lines are fitted trend lines.

Table 6 *Regression Models for Fouling Resistance (R_f)* Fitted to the Twelve Monthly Cases

Predictor	Model form	Fitted equation	R^2	p (slope)
Time, t (months)	Power	$R_f = 0.0237\ t^{0.0441}$	0.951	< 0.001
U (W/m²·°C)	Power	$R_f = 3.5006\ U^{-1.792}$	0.986	< 0.001
LMTD (°C)	Linear	$R_f = 0.002$ LMTD − 0.0892	0.777	< 0.001
(kg/s)	Logarithmic	$R_f = 0.004$ ln( ) + 0.0046	0.902	< 0.001

Note. $n = 12$ for all models. R^2 and p values were computed from the data in Table 4. The 95% confidence interval of the exponent is 0.037–0.051 for time and −1.944 to −1.644 for U; that of the slope is 0.0013–0.0028 for LMTD and 0.0031–0.0050 per unit ln( ).

Fouling resistance increased with both LMTD and mass flow rate (positive slopes). Two features of the data limit how these relationships should be read. First, mass flow rate was increased by exactly 10 kg/s each month, so mass flow rate and time are perfectly collinear ($r = 1.00$); the logarithmic relationship in Table 6 therefore reflects the progression of fouling with time and cannot be attributed to flow rate itself. Second, LMTD takes essentially only two values (about 55.40 °C in months 1–2 and 56.35 °C in months 3–12; Figure 4c), so the linear LMTD fit is driven by two clusters of points and has limited predictive meaning.

4.3 Discussion

The simulated results are consistent with the established understanding that fouling lowers the overall heat transfer coefficient and thereby reduces heat duty and cooling effectiveness (Lebele-Alawa & Innocent, 2020; Ogbonnaya & Ajayi, 2017; Ogbonnaya et al., 2020). The finding that fouling resistance grows with time at a decreasing rate agrees with the timedependent fouling behaviour reported from operating plants, in which resistance rises as deposits accumulate while efficiency falls (Ogbonnaya et al., 2020; Pullela et al., 2020). The close power-law relationship between R_f and U is largely algebraic, since R_f is computed from U_s (Eq. 6), but it is useful operationally because U_s can be inferred routinely from temperature and flow measurements, so a fouling resistance can be estimated without opening the exchanger.

The mass flow rate result requires caution. In the literature, a higher flow velocity generally increases wall shear stress and removal, lowering the fouling rate for many mechanisms (Jradi et al., 2022b). The positive association between R_f and mass flow rate in this study

should therefore not be read as evidence that higher flow worsens fouling; it arises from the simulation design, in which flow and time were varied together. Separating the effects would require simulating several flow rates at the same fouling state, and several fouling states at the same flow rate. Similarly, the decrease in hydrocarbon velocity with time (0.615 to 0.593 m/s) is consistent with a progressively blocked flow area and, in a real exchanger, would be accompanied by a growing pressure drop and pumping power, which should be quantified in future simulations (Kazi, 2020; Tutpol et al., 2023).

The absolute values should also be interpreted with care. The simulated fouling resistance (about 0.024 $m^2 \cdot °C/W$) is far larger than typical TEMA design allowances, which are of the order of 10^{-4} $m^2 \cdot °C/W$, and the simulated hydrocarbon outlet temperatures (74–79 °C) differ from the design outlet temperature of 48.9 °C. The simulated model therefore operates at conditions different from the design case, and its R_f and U values are best used as relative indicators of the trend in fouling, rather than as absolute design values.

From a maintenance perspective, the regression relationships offer a simple basis for estimating fouling growth and for setting a cleaning threshold, for example by triggering cleaning when the estimated R_f, or the fall in U, reaches a limit set by the allowable outlet temperature of the hydrocarbon. Fouling mitigation measures that operators may consider include controlling foulant concentration and fluid composition, chemical additives, online mechanical cleaning, maintaining adequate velocity and low wall temperature, periodic chemical or mechanical cleaning, and surface coatings and treatments (BenMansour et al., 2023; Kazi, 2020).

4.4 Limitations

The study has several limitations. The monthly progression of fouling was simulated rather than measured over successive months of plant operation, and the simulation outputs were not compared with measured plant data, so the results are not yet validated. Flow rate and time were varied together, so their effects are confounded, and LMTD took only two distinct values. Only twelve data points from one exchanger were used, and the regression fits were single-variable. Pressure-drop results, detailed solver settings and mesh statistics are not reported here. Fouling was not resolved by mechanism, and the effects of foulant

composition and thermal conductivity were not investigated. A cost or downtime optimisation of cleaning was not performed.

5. Conclusions and Recommendations

5.1 Conclusions

Fouling in a shell-and-tube heat exchanger cooling a hydrocarbon stream with water was modelled and simulated in ANSYS 14.0, using plant design and operating data. The main conclusions are as follows:

In the first simulated month, fouling reduced heat duty by 36.25% relative to the clean exchanger, raised the hydrocarbon outlet temperature from 70.5 °C to 74.2 °C and lowered the overall heat transfer coefficient from 26.26–27.02 to 16.15 W/m²·°C. Over twelve simulated monthly cases, fouling resistance rose from 0.0238 to 0.0264 m²·°C/W while U fell from 16.15 to 15.24 W/m²·°C, showing that exchanger efficiency diminishes as fouling resistance increases with time. Fouling resistance was strongly related to the overall heat transfer coefficient (power law, $R^2 = 0.986$), time (power law, $R^2 = 0.951$) and mass flow rate (logarithmic, $R^2 = 0.902$), and moderately to LMTD (linear, $R^2 = 0.777$). Because flow rate and time were varied together, only the dependence on time and U can be interpreted with confidence. The relationships developed provide a simple, transparent basis for forecasting fouling growth and planning cleaning of this type of exchanger, subject to validation against plant data.

5.2 Recommendations and Future Work

The following are recommended:

(i) Validation of the simulation against measured plant temperatures, flows and pressure drops;

(ii) Independent variation of flow rate, temperature and fouling-layer thickness, so that their effects can be separated;

(iii) Multiple regression or machine-learning models with proper statistical diagnostics;

(iv) Inclusion of pressure-drop and pumping-power effects;

(v) Cost-based optimisation of cleaning schedules; and

(vi) Application to additional exchangers and fluids. Operators should monitor *U* and outlet temperatures routinely and consider fluid composition, contaminants, process conditions, exchanger configuration and surface temperature in managing fouling.

5.3 Contribution to Knowledge

The study contributes a documented ANSYS-based simulation of an in-service BEM shelland-tube exchanger, an assessment of its fouling behaviour at different operating conditions, and regression relationships linking fouling resistance to the overall heat transfer coefficient, time, mass flow rate and LMTD for use in performance monitoring and maintenance planning.

REFERENCES

1. Anand, P. (2023). Heat exchangers in industrial applications: Efficiency and optimization strategies. *International Journal of Engineering Research and Technology, 12*(9), 1–10.

2. Ben-Mansour, R., El-Ferik, S., Al-Naser, M., Qureshi, B. A., Eltoum, M. A. M., Abuelyamen, A., Al-Sunni, F., & Ben Mansour, R. (2023). Experimental/numerical investigation and prediction of fouling in multiphase flow heat exchangers: A review. *Energies, 16*(6), Article 2812. https://doi.org/10.3390/en16062812

3. Diaz-Bejarano, E., Coletti, F., & Macchietto, S. (2020). A model-based method for visualization, monitoring, and diagnosis of fouling in heat exchangers. *Industrial & Engineering Chemistry Research, 59*(10), 4602–4619. https://doi.org/10.1021/acs.iecr.9b05490

4. Fernandes, E. J., & Krishanmurthy, S. H. (2022). Design and analysis of shell and tube heat exchanger. *International Journal for Simulation and Multidisciplinary Design Optimization, 13*, Article 15. https://doi.org/10.1051/smdo/2022005

5. Ishiyama, E. M., Paterson, W. R., & Wilson, D. I. (2020). The effect of fouling on heat transfer, pressure drop and throughput in refinery preheat trains: Optimisation of cleaning schedules. In *Proceedings of the 7th International Conference on Heat Exchanger Fouling and Cleaning*. Engineering Conferences International.

6. Jradi, R., Marvillet, C., & Jeday, M. R. (2022a). Application of artificial neural network method for prediction of tube-side fouling resistance in shell-and-tube heat exchanger. *Fluid Dynamics & Materials Processing*. https://doi.org/10.32604/fdmp.2022.021925

7. Jradi, R., Marvillet, C., & Jeday, M. R. (2022b). Fouling in industrial heat exchangers: Formation, detection and mitigation. *IntechOpen*. https://doi.org/10.5772/intechopen.102487

8. Kazi, S. N. (2020). Fouling and fouling mitigation of calcium compounds on heat exchangers by novel colloids and surface modifications. *Reviews in Chemical Engineering, 36*, 653–685.

9. Kern, D. Q., & Seaton, R. E. (1959). A theoretical analysis of thermal surface fouling. *British Chemical Engineering, 4*(5), 258–262.

10. Lebele-Alawa, B. T., & Innocent, O. O. (2020). Influence of fouling on heat exchanger effectiveness in a polyethylene plant. *Energy and Power, 4*(2), 29–34.

11. Lee, H. H. (2017). *Finite element simulations with ANSYS Workbench 17*. SDC Publications.

12. Loyola, F. J. (2019). Estimation of fouling model parameters for shell side and tube side of crude oil heat exchangers using data reconciliation and parameter estimation. *Industrial & Engineering Chemistry Research*. https://doi.org/10.1021/acs.iecr.9b00457

13. Müller-Steinhagen, H. (2011). Heat transfer fouling: 50 years after the Kern and Seaton model. *Heat Transfer Engineering, 32*(1), 1–13. https://doi.org/10.1080/01457632.2010.505127

14. Nadra, H., Hassan, A. I., & Ahmad, S. (2020). Modelling of fouling in heat exchangers using the artificial neural network approach. *International Journal of Chemistry, Mathematics and Physics, 2*(5), 33–55.

15. Ogbonnaya, S. K., & Ajayi, O. O. (2017). Fouling phenomenon and its effect on heat exchanger: A review. *Frontiers in Heat and Mass Transfer, 9*, Article 31. https://doi.org/10.5098/hmt.9.31

16. Ogbonnaya, S. K., Ajayi, O. O., Ohijeagbon, O. D., & Ogbonnaya, M. (2020). Modeling and analysis of fouling behaviour in plate and frame heat exchanger. *Covenant Journal of Engineering Technology, 2*(2), 72–80.

17. Paul, B. T. (2019). Operation of a shell and tubes heat exchanger: Process simulation. *Contemporary Engineering Sciences, 12*(3), 131–147.

18. Pullela, K. S., Ramakrishna, K., Tunuguntla, S., Lankapalli, S. V., Prasad, V. S., Korada, V. S., Dharma, R. V., & Veerapanen, S. R. K. P. (2020). Fouling and its effect on the thermal performance of heat exchanger tubes. *International Journal of Heat and Technology, 35*(3), 509–519. https://doi.org/10.18280/ijht.350307

19. Rehman, O. U., Ramasamy, M. G., Rozali, N. E. M., Mahadzir, S., Ghumman, A. S. M., & Qureshi, A. H. (2023). Modeling strategies for crude oil-induced fouling in heat exchangers: A review. *Processes, 11*(4), Article 1036. https://doi.org/10.3390/pr11041036

20. Sharma, A., & Macchietto, S. (2021). Fouling and cleaning of plate heat exchangers: Dairy application. *Food and Bioproducts Processing, 126*, 32–41.

21. Sundar, S., Rajagopal, M. C., Zhao, H., Kuntumalla, G., Meng, Y., Chang, H. C., Shao, C., Ferreira, P., Miljkovic, N., Sinha, S., & Salapaka, S. (2020). Fouling modeling and prediction approach for heat exchangers using deep learning. *International Journal of Heat and Mass Transfer, 159*, Article 120112.

22. Swanand, G., & Ashish, P. (2021). Numerical simulation of the effect of baffle cut and baffle spacing on shell side heat exchanger performance using CFD. *Chemical Product and Process Modeling, 16*(2), 145–154.

23. Tutpol, A., Wesley, H., & Belle, R. U. (2023). Heat exchanger fouling and estimation of remaining useful life. *Annual Conference of the Prognostics and Health Management Society*, Knoxville, TN, USA.

24. Wu, X., Ze, H., Xiaobin, J., Xiangcun, L., Xuemei, W., & Gaohong, H. (2019). Heat exchanger reliability analysis based on fouling growth model by fault tree analysis. *Chemical Engineering Transactions, 76*, 265–270.

25. Yang, Z., Ma, Y., Zhang, N., & Smith, R. (2020). Design optimization of shell and tube heat exchangers sizing with heat transfer enhancement. *Computers & Chemical Engineering, 137*, Article 106821. https://doi.org/10.1016/j.compchemeng.2020.106821

26. Zahid, K., Patel, R., & Mujtaba, I. M. (2016). Development of a dynamic fouling model for a heat exchanger. *Chemical Engineering Transactions, 52*, 1135–1140. https://doi.org/10.3303/CET1652190